Hydrol. Earth Syst. Sci. Discuss., 10, 9271–9308, 2013
www.hydrol-earth-syst-sci-discuss.net/10/9271/2013/
doi:10.5194/hessd-10-9271-2013

Hydrology and Earth System Sciences
Open Access
Discussions

Water balance and its intra-annual variability in a permafrost catchment: hydrological interactions between catchment, lake and talik

E. Bosson[1,2], T. Lindborg[2,3], S. Berglund[4], L.-G. Gustafsson[5], J.-O. Selroos[1,2], H. Laudon[3], L. L. Claesson[2], and G. Destouni[1]

[1]Department of Physical Geography and Quaternary Geology, Bert Bolin Centre for Climate Research, Stockholm University, 106 91, Stockholm, Sweden
[2]Swedish Nuclear Fuel and Waste Management Co, Box 250, 101 24, Stockholm, Sweden
[3]Department of forest ecology and management, Swedish University of Agricultural science, 90183 Umeå, Sweden
[4]Hydroresearch AB, St. Marknadsvägen 15S (12th floor), 18334, Täby, Sweden
[5]DHI Sweden AB, Lilla Bommen 1, 411 04 Gothenburg, Sweden

Received: 25 June 2013 – Accepted: 2 July 2013 – Published: 16 July 2013

Correspondence to: E. Bosson (emma.bosson@skb.se)

Published by Copernicus Publications on behalf of the European Geosciences Union.

Abstract

Few hydrological studies have been made in Greenland with focus on permafrost hydrology rather than on the glacial hydrology associated with the Greenland ice sheet. Understanding permafrost hydrology, and its reflection and propagation of hydroclimatic change and variability, however, can be a key to understand important climate change effects and feedbacks in arctic landscapes. This paper presents a new extensive and detailed hydrological dataset, with high temporal resolution of main hydrological parameters, for a permafrost catchment with a lake underlain by a talik close to the Greenland ice sheet in the Kangerlussuaq region, western Greenland. The paper describes the hydrological site investigations and data collection, and their synthesis and interpretation to develop a conceptual hydrological model. The catchment and lake water balances and their intra-annual variability, and uncertainty intervals for key water balance components, are quantified. The study incorporates all relevant hydrological processes within the catchment and, specifically, links the surface water system to both supra-permafrost and sub-permafrost groundwater. The dataset enabled water balance quantification with high degree of confidence. The measured hydraulic gradient between the lake and the groundwater in the talik shows this to be a groundwater recharging talik. Surface processes, dominated by evapotranspiration during the active flow period, and by snow dynamics during the frozen winter period, influence the temporal variation of groundwater pressure in the talik. This shows the hydrology in the catchment as being rather independent from external large-scale landscape features, including those of the close-by ice sheet.

1 Introduction

The water balance of arctic and sub-arctic regions is influenced by ice, snow and frozen soil with large seasonal fluctuations in the surface energy balance (Woo et al., 2008). Hydrological responses in these high latitude areas differ in fundamental aspects from

HESSD
10, 9271–9308, 2013

catchments in boreal and temperate regions (Kane et al., 2004). One such difference is that the hydrological cycle in cold regions is intimately connected to the presence of permafrost (White et al., 2007), which controls the distribution and routing of water across the landscape (Quinton and Carey, 2008) and other hydrological processes within a catchment (Woo, 1986). The hydrologically active period with water flowing on the ground surface and in the active layer is relatively short. Snowmelt is often the main hydrological event of the year, emphasizing the necessity of including winter and spring measurements in the water balance assessments (Hirashima et al., 2004). Furthermore, sublimation has been shown to be significant in the water balance of cold region environments (Reba et al., 2011; McDonald et al., 2010).

Groundwater recharge and discharge are reduced by the presence of permafrost but both computational (Bense et al., 2009; Frampton et al., 2011, 2013; Ge et al., 2011; Grenier et al., 2012; Bosson et al., 2012b) and observational studies (Kane et al., 2012) indicate their importance. Water exchange of deep and shallow groundwater through taliks – unfrozen soil or bedrock underlying lakes – needs to be taken into consideration in water balance assessments for catchments with permafrost. A modelling study performed by Bosson et al. (2012a) showed the complexity in the connections between different hydrological flow and storage components of a catchment under different climate, landscape and permafrost states. The study emphasized the need of linking subsurface hydrology to surface processes and taking the permafrost component into account to better understand and describe hydrological processes in cold regions.

Hinzman et al. (2012) summarized the current status of progress in the research of hydrogeology in cold regions, including regional (Cheng et at al., 2012), process (Sjöberg et al., 2012) and simulation (Frampton et al., 2012; Wellman et al., 2012; McKenzie and Voss, 2012) investigations of long-term changes to permafrost hydrology. However, few studies focus on the short-term variability of hydrological processes in permafrost environments. The water balance of the active layer (Helbig et al., 2012) and its hydrological response to a changing climate (Quinton and Baltzer, 2012) have been investigated but, to our best knowledge, few previous studies have considered

HESSD
10, 9271–9308, 2013

all relevant catchment processes, including also the links and interactions between subsurface and surface water.

The present study focuses on the short-term (intra-annual) variability of the linked surface and subsurface hydrological processes in an arctic permafrost catchment in western Greenland, for which we present a new hydrological dataset. The extent of the dataset, containing all relevant processes on the catchment scale, enables quantification of the water balance with a high degree of confidence. The data set also links surface waters to both supra-permafrost and sub-permafrost groundwater. The study aims to: (i) quantify the water balance of the catchment, and its associated lake talik, and (ii) construct a conceptual model of this whole hydrological system that can be used as basis for further modeling of permafrost hydrology and permafrost environments in general.

In the following, we present in Sect. 2 the investigated site, the hydrological data collection and analysis, and the methodology for water balance assessment. In the results Sect. 3, the conceptual model together with a water balance for the lake and surrounding catchment for the hydrological year 2011–2012 is presented. In Sect. 4, we further discuss the processes accounted for and associated uncertainty intervals. Main conclusions from the study are finally summarized in Sect. 5.

2 Material and methods

2.1 Site description

The study site, here referred to as the Two Boat Lake (TBL) catchment, is situated approximately 25 km North East of the settlement Kangerlussuaq, in West Greenland. This is the most extensive ice free part of Greenland, which includes a broad range of arctic environments, from the coast, through plains and a hilly terrain, towards the ice sheet margin (see Fig. 1). The study site consists of a lake-centred catchment area (see geometric data in Table 1) and is located close to (500 m from) the Greenland

HESSD
10, 9271–9308, 2013

ice sheet. However, the site is not a part of the melt water runoff system. Relatively stable high-pressure cells over the ice sheet dominate the regional climate, which are further strengthened by catabatic winds so that easterly wind directions dominate the regional wind patterns. Low-pressure systems and associated precipitation arrive from the south-west, but a substantial portion of the moisture is precipitated over the Sukkertoppen Ice Cap (Fig. 1), yielding a more continental climate at Kangerlussuaq (Engels and Helmens, 2010). A gradient of decreasing precipitation, P, is observed from the coast towards the inland. Mean annual P at the station in Kangerlussuaq (Fig. 1) is 173 mm (measured 1977–2011), of which 67 mm is snow and 106 mm is rain. This is a desert-like annual precipitation. Mean annual temperature in Kangerlussuaq is –5.1 °C ranging from –9.1 to –0.3 °C (measured 1977–2011; Cappelen ed., 2012).

The catchment area of TBL is dominated by till and glaciofluvial deposits (Fig. 1), which to a large part are overlain by a layer of Eolian silt to fine sand. The total depth of Eolian sediments and glacial deposits ranges from 7–12 m in the valleys to zero along the hill sides. In the lake, a sediment thickness up to 1.5 m has been observed (Petrone, 2013). It is assumed that the observed depth of glacial deposits in the valleys of the catchment is also present in the lake, i.e., the lake sediments are underlain by approximately 10 m of till. The till and glaciofluvial deposits were deposited close to the ice front during deglaciation of the area. The eolian silt to fine sand has periodically been deposited after the area was deglaciated (Willemse et al., 2003).

In general, vegetation in the TBL catchment is dominated by dwarf-shrub heath. There are no trees, and bushes rarely exceed a height of 0.5 m. The poor vegetation results in a relatively low transpiration even though the total evapotranspiration is relatively high in the area compared to other water balance components. The only visible stream furrow is that in the outlet of the lake. Depressions formed by ice wedges are the major transport ways of water from the catchment to the lake. Due to the low precipitation in the area, the stream at the outlet of the lake is dry during long periods and the summer of 2009 was the last time surface water outflow was observed to occur from the lake. The surface water divide is well defined around the catchment and the

HESSD
10, 9271–9308, 2013

groundwater divide in the active layer is assumed to coincide with it. However, in a valley in the northern part of the catchment (Fig. 1), the topographical gradient is small and the groundwater divide might change in time depending on the thawed depth of the active layer.

A digital elevation model (DEM) for the TBL catchment was developed and reported by Clarhäll (2011). The DEM describes both the catchment topography and the lake bathymetry, and geometrical parameters extracted from the DEM are summarized in Table 1. The DEM confirms that the TBL catchment hydrology is a precipitation-driven system, with no melt water inflow from the glacier occurring over the catchment boundary. Drilling has confirmed the presence of a talik below the lake, which allows for hydraulic contact with the deep groundwater system below the permafrost. Continuous permafrost interrupted by through taliks covers the regional area, and permafrost depth more than 300 m is indicated by temperature measurements in deep boreholes in the vicinity of the lake (Harper et al., 2011).

2.2 From data collection to conceptual model

The methodology employed for constructing a conceptual hydrological model of the TBL area, and calculating the water balance of its catchment is illustrated in Fig. 2. All available relevant data from the site was used in the analysis and conceptualisation (Fig. 2a and b). The water balance for the lake was first calculated on an annual basis (Fig. 2c) and then temporal variations of the parameters were analysed (Fig. 2d). By using time series of precipitation (P), potential evapotranspiration (PET) and lake level fluctuation (ΔH), a time series of runoff (R) from the catchment to the lake was calculated. Based on specific events in the time series of R, uncertainty intervals for the annual sums of P on the lake, evaporation (E) from the lake and R were determined (Fig. 2e). Finally, the water balance for the lake was used to calculate the water balance of its catchment (Fig. 2f). In the following sections, the steps corresponding to each box in Fig. 2a–f are described.

HESSD
10, 9271–9308, 2013

2.2.1 Instrumentation and data collection

Hydrological investigations and instrumentation in the TBL catchment area, performed during the period 2010–2012, have resulted in a dataset covering meteorological and hydrological conditions, soil temperature and hydraulic properties of the active layer (Figs. 1, 2a, Table 2). A local Automatic Weather Station (AWS) and a time-lapse camera was installed in the catchment to monitor the hydrological and meteorological events during the year. Soil moisture in the catchment is monitored by Time Domain Reflectometry Technique (TDR) in three clusters (Fig. 1). Soil sampling in the area has generated data on total porosity for each representative type of regolith material and for all the sites where TDR sensors were installed.

2.2.2 Data analysis and conceptualization

Meteorological data

Measured precipitation data had to be corrected due to gauge undercatch caused by wind and adhesion losses. The correction factors used for the TBL catchment (Table 3) are based on the location and wind exposure of the weather station (Alexanderson, 2003), and are of the same order of magnitude as those used reported from other studies in Greenland, e.g. Hasholt (1997); Førland et al. (1996). The monthly mean temperature, PET and corrected *P* from the AWS are presented in Table 3. Data from the station in Kangerlussuaq (Fig. 1) is also presented in the table in order to relate the AWS data to the long-term records in Kangerlussuaq. In this study, the hydrological year from 1 September 2011 to 31 August 2012 is evaluated: the observed total corrected *P* at the AWS during this period was 260 mm, Table 3. The dominating wind direction was from southeast (Fig. 3) carrying cold dry air from the ice sheet.

Figure 4 illustrates snow accumulation and melting expressed as mm snow water equivalents (SWE). Snow accumulates from October and melts from March to May. Snow depth measurements performed in April 2011 (Fig. 1) indicated an irregular

HESSD
10, 9271–9308, 2013

snow cover, with snow accumulation in the valleys, and snowdrift in wind exposed areas at the hillsides and on high topographical points. The mean threshold wind speed for snowdrift (Li and Pomeroy, 1997) is frequently exceeded. It was calculated to be 8 m s^{-1}, ranging from 7 to 11 m s^{-1} depending on air temperature. In April 2013, sublimation measurements were performed at three sites in the catchment (Fig. 1) resulting in a mean sublimation rate of 2.75 mm day^{-1} for the observed period. For a more detailed description of the meteorological conditions and sublimation measurements, see Supplement Sect. 1.1.

Active layer and lake ice

Results from the monitoring (Fig. 3) indicate that the deepest active layer depth during 2010–2012 was 0.9 m. This is within the range of the measurements performed in catchment transects (Clarhäll, 2011), suggesting a mean depth of the active layer of 0.7 m. The active layer reaches its maximum depth in late August–early September. The different periods of frozen and active conditions in the TBL catchment were defined based on soil temperature and water content data (see Supplement, Sect. 1.2), Table 4. Lake freezing occurred in October when the monthly mean air temperature was −8 °C and the lake ice started to melt in late April. The ice reached a maximum thickness of approximately 1.6 m during the winter season 2011/2012.

Lake level measurements

The surface water pressure in the lake is monitored by two absolute pressure transducers placed at the bottom of the lake. This means that the pressure data must be corrected for barometric effects, which is done using air pressure data from the AWS. Corrected data was expressed in meters of water (Fig. 4a). The lake level never exceeded its threshold level (which been defined and measured by using a leveling instrument) for surface water outflow during the observed period. A more extensive description of the lake pressure variations is given in Supplement Sect. 1.3.

HESSD
10, 9271–9308, 2013

In 2012, three larger snowmelt events were observed (Fig. 4a and b). However, monitoring data showed that the first lake-level response to snowmelt took place during the third snowmelt event, in May 2012, when the uppermost part of the active layer had thawed. The water from the two initial snowmelt events formed small ponds of water, isolated due to the frozen ground surface, Fig. 4c. The ponds re-froze as the temperature dropped during certain periods in March and April. As the uppermost soil layer thawed, the "thresholds" of the ponds disappeared and the water could flow to the lake, causing a lake-level rise, (Fig. 4d).

Soil moisture data and porosity

Due to the high *P* recorded during 2012, both at TBL and in Kangerlussuaq (compared to long term mean values) the change in soil moisture content was taken into consideration. TDR data were evaluated in order to determine the change in total water content in the active layer during the hydrological year. Based on the distribution of regolith, and the location of the TDR sensors, the total storage change was calculated to be 15 mm (17 555 m^3); for a detailed description of the calculation see Supplement Sect. 1.4.

Borehole data

A 221 m long borehole, DH-GAP01 (Fig. 1), was drilled in a 60° inclination under the TBL, reaching a vertical depth relative to the top of casing (TOC) of 191.5 m. Hydraulic pressure was measured at a vertical depth of 138.57 m (relative to the TOC, for details see Supplement Sect. 1.5). Based on temperature data from the borehole, the upper 20 m of the borehole is considered to be in permafrost. The transition from frozen to unfrozen ground coincides with the lake shoreline, i.e., temperature data indicates a talik being maintained under the lake. The mean temperature in the bedrock under the lake is 1.25 °C. The mean difference in hydraulic head over the hydrological year was calculated to be 1.85 m, implying a mean hydraulic gradient of 0.014 with a downward direction (i.e., recharge flow into the talik). A hydraulic test was performed in DH-GAP01

HESSD
10, 9271–9308, 2013

in the summer of 2010 and the mean hydraulic conductivity of the bedrock below the lake was calculated to be 2–5 × 10^{-8} m s^{-1} (Harper et al., 2011).

2.3 Lake water balance calculations

The water balance for the catchment was calculated in two steps. First, the water balance for the lake was determined. Based on this result, the water balance for the lake catchment was further calculated. A base case for the lake water balance was calculated by Eq. (1) (Fig. 2c):

$$(P - \Delta H) - E + R = 0 \quad (1)$$

where P is precipitation, ΔH is the difference in lake level (under the assumption that the lake area is constant), E is the evaporation from the lake and R is net total runoff (i.e total inflow minus total outflow from the lake). P and ΔH were measured in the catchment area and E is in the base scenario assumed to be equal to the calculated PET (which is based on local data from the AWS). The runoff can be divided into four terms: Rs_{in}, Rs_{out}, R_{gw} and R_{al}, where Rs is the surface water runoff to/from the lake, R_{al} is the groundwater exchange in the active layer (negative out from the lake) and R_{gw} is the lake water exchange with the groundwater in the talik below the lake (negative downwards from the lake). During the studied period the lake level never exceeded the level of the lake threshold; thus, Rs_{out} can be set equal to zero and Eq. (1) can be rewritten as:

$$(P - \Delta H) - E + \left(R_{al} + Rs_{in} + R_{gw}\right) = 0 \quad (2)$$

R_{gw} is calculated with Darcy's law:

$$R_{gw} = K \cdot \frac{dh}{dZ} \quad (3)$$

HESSD
10, 9271–9308, 2013

where K ($\mathrm{m\,s^{-1}}$) is the hydraulic conductivity of the bedrock under the lake and $\frac{dh}{dZ}$ is the mean hydraulic gradient between the lake and the groundwater pressure observation point in the borehole over the studied period.

Based on the calculated annual sum of R_{al} and Rs_{in} for the lake, the water balance for the lake catchment can further be calculated by Eq. (4) (Fig. 2f):

$$P - ET - Rs_{in} - R_{al} + \Delta S_{al} = 0 \quad (4)$$

where P is the corrected measured precipitation at the AWS, ET is the evapotranspiration from the catchment and ΔS_{al} is the change in storage in the active layer. Storage change in the permafrost is assumed to be zero over the studied hydrological year. Equation (4) can be solved for ET since P is measured, the sum ($Rs_{in} + R_{al}$) is calculated by Eq. (2), and the change in storage in the active layer is given from soil moisture measurements.

3 Results

3.1 Conceptual model of the TBL catchment

The conceptual hydrological model was established (Figs. 2b, 5) based on all available data. The flow paths of water within the catchment change throughout the year, so that two conceptual model parts needed to be developed: one for the frozen period and one for the active period (Table 4).

During the active period, surface water flow to and from the lake, R_s, as well as a groundwater exchange with the lake in the active layer, R_{al}, and the talik, R_{gw}, may occur. In the beginning of the active period, when temperature fluctuates around 0 °C, melt water from snow forms small ponds on the frozen ground surface, which refreezes before the melt water reaches the lake as the uppermost soil layer thaws. Precipitation which comes as rain is assumed to be uniformly distributed in the catchment during the active period and equal to that measured at the AWS.

HESSD
10, 9271–9308, 2013

In the frozen period no surface water flow occurs and once the lake ice has reached a thickness greater than the active layer, there is no water exchange between the lake and the surrounding active layer. The frozen water in the permafrost and the saturated parts of the active layer is assumed to be immobile. Groundwater exchange with the talik, R_{gw}, is possible. If the active layer is unsaturated at the time of soil freezing (Table 4), lake water might flow into the unsaturated parts of the active layer in response to an increased water pressure in the lake; this process can occur only as long as the lake ice has not reached the thickness of the active layer.

Snowdrift, resulting in snow redistribution, and snow mass loss via snow sublimation influence the water balance. Losses and gains of catchment water due to snow drift over the catchment boundary are assumed to equal each other.

3.2 Lake water balance, base case

For the studied hydrological year, $P = 260$ mm, PET = 413 mm and ΔH is 73 mm, resulting in $R = 226\,\mathrm{mm\,yr^{-1}}$ by solving Eq. (1). R_{gw}, calculated by Eq. (3), has an average value of $-15\,\mathrm{mm\,yr^{-1}}$ (-9 to $-21\,\mathrm{mm\,yr^{-1}}$, depending on which K value used), which implies a net outflow of water from the lake to the groundwater in the underlying talik. With $R_{gw} = -15\,\mathrm{mm\,yr^{-1}}$, the net annual inflow of water to the lake from the catchment, via R_{al} and Rs_{in}, is calculated to be 241 mm.

To identify hydrological events during the year, a time series of R was calculated by Eq. (1) based on the daily precipitation and lake-level measurements, and the calculated time series of PET (Figs. 6 and 2d). To reduce the noise of shorter-term variations, a seven-day running average was applied to the time series of lake level fluctuations (ΔH) in the calculations. Figure 6 shows that R is then negative during certain periods of the year (implying net outflow of water from the lake), even though the net R for the whole year is positive. Shorter periods of negative R during the active period are due to the flow sum of R_{al} and R_{gw} being directed out from the lake during periods of high ET and/or low P in the catchment. Negative R can also be observed periodically

HESSD
10, 9271–9308, 2013

during November to March, when the lake is ice covered (Table 4, Fig. 6). According to the conceptual model defining the base case (Fig. 5), flow paths via R_{al} and Rs are closed when the system is fully frozen. The negative calculated R under this period could then only be associated to R_{gw}. However, the base parameterisation of the talik bedrock properties implies that the calculated negative R cannot consist of R_{gw} only. The negative R identified for the frozen period was then used as a basis for estimating uncertainty intervals for key parameters in the water balance equation, as discussed further below (Fig. 2e).

3.3 Estimation of uncertainty intervals for P, E and R_{al}

The total net R for the frozen period from 1 November until 31 March is calculated to be −30 mm (Fig. 6). The average R_{gw} for the same period is −8 mm. Since Rs and R_{al} are assumed to be zero during the frozen period (Fig. 5) the resulting net R of −22 mm implies a water balance error, which in turn indicates that other processes, not captured in the base case, influence the water balance during this part of the frozen period.

To identify processes not accounted for, which could explain the negative R during the frozen period 1 November–31 March, three alternative cases, differing from the base case, are analysed and uncertainty intervals are estimated for the components P, E and R. In the first case, the influence of snowdrift on P is analysed. In the second case the influence of sublimation on E is analysed. In the third case the influence of groundwater exchange in the talik on R is analysed. The uncertainty intervals of P, E and R determined from each case imply a range of different annual sums of each parameter, which is further considered in the total water balance of the lake and its catchment.

In the calculations of cases 1–3, the sums of P, PET, R_{gw} and ΔH for the frozen period 1 November–31 March conditions are denoted with index fp, where P_{fp} = 56 mm, PET_{fp} = 19 mm, R_{fp} = −30 mm, $R_{gw\text{-}fp}$ = −8 mm and ΔH_{fp} = 8 mm.

HESSD
10, 9271–9308, 2013

3.3.1 Case 1: Assumptions: (a) R_{al} and Rs are zero during the frozen period, and (b) snowdrift occurs with wind events on the lake

Assumptions (a) and (b) imply that the calculated negative R is wrong and the error is in the P term due to the wind drift of snow, i.e., the measured P at the AWS is not correct for the lake during the frozen period. The observed P_{fp} at the AWS consists of 6 mm rain and 50 mm SWE. To calculate the actual amount of snow and rain falling on the lake during the frozen period, Eq. (2) is solved for P_{lake}:

$$(P_{lake} - \Delta H) - E + (R_{gw}) = 0$$

$$P_{lake} = E + \Delta H - R_{gw} = 19 + 8 - (-8) = 35$$

P_{lake} is calculated to be 35 mm, and the observed 6 mm of rain is assumed to stay on the lake, which implies that only 29 mm of the observed 50 mm SWE remains on the lake while the rest, 21 mm SWE, moves into the catchment due to the wind drift of snow. The actual annual P for the lake area is then calculated by Eq. (5), where P_{aws} is the total annual observed precipitation at the AWS and $P_{winddrift}$ is the amount of snow blowing away from the lake, expressed in SWE (21 mm). In case 1, under assumptions (a) and (b), the total P for the hydrological year of the lake area is calculated to be 239 mm according to Eq. (5):

$$P = P_{aws} - P_{winddrift} \quad (5)$$

3.3.2 Case 2: Assumptions: (c) R_{al} and Rs are zero during the frozen period, and (d) Snow sublimation is underestimated

Assumptions (c) and (d) imply that the calculated negative R is wrong and the error is in the E term due to an underestimation of snow sublimation. To calculate total evaporation including snow sublimation for the frozen period, Eq. (2) was solved for E:

$$(P_{fp} - \Delta H_{fp}) - E_{fp} + (R_{gw\_fp}) = 0$$

$$E_{fp} = P_{fp} - \Delta H_{fp} + R_{gw\_fp} = 56 - 8 + (-8) = 40$$

HESSD
10, 9271–9308, 2013

$E_{fp} - PET_{fp}$ gives then an indication of the extra snow sublimation, not included in the original time series of PET, being equal to 21 mm (40–19).

The actual total E from the lake for the whole hydrological year is then calculated by adding the extra winter evaporation (sublimation from snow) for the frozen period to the annual PET. In case 2, under assumptions (c) and (d), the annual E is calculated to be 434 mm.

3.3.3 Case 3: Assumption: (e) R_{gw} is underestimated due to an underestimated K value for the bedrock.

The K values determined by hydraulic tests in DH-GAP01 result in R_{gw_fp} ranging from 4.6–11.5 mm. An analysis was performed to estimate the K value needed to obtain a higher R_{gw} value, so that the total negative R for the frozen period in the base scenario could be associated only with R_{gw}. The calculated R_{fp} of −22 mm corresponds to a mean Darcy velocity of $2.3 \times 10^{-9}\,m\,s^{-1}$. The mean head difference between the lake and talik for the frozen period is 2.24 m so that Eq. (3) can be solved for K (with $dz = -128.1$ m). In case 3, under assumption (e) a K value for the bedrock of $1.3 \times 10^{-7}\,m\,s^{-1}$ (compared to $2–5 \times 10^{-8}\,m\,s^{-1}$ in the base case) yields a total R_{gw} of −54 mm for the whole hydrological year.

$$K = R_{gw} \cdot \frac{dz}{dh} = 1.3 \times 10^{-7}$$

The cases 1–3 along with the base case give uncertainty intervals for P, E and R in the total annual water balance of the lake presented in Fig. 7. Since Rs_{in} is not explicitly measured, Rs_{in} and R_{al} cannot be separated. The flows are expressed in $m^3\,yr^{-1}$ assuming a constant surface area of the lake of 377 900 m^2. The annual precipitation falling on the lake ranges from 90 320 to 98 255 m^3 (239–260 mm), E ranges from 156 070 to 164 010 m^3 (413–434 mm), R_{gw} ranges from −5670 to −20 410 m^3 (−15 to −54 mm), and ($R_{al} + R_{in}$) ranges from 91 075 to 105 810 m^3 (241–280 mm). The water

HESSD
10, 9271–9308, 2013

exchange with the underlying talik is then around 15 % of the net inflow ($R_{al} + Rs_{in}$) from the lake catchment. The evaporation from the lake is the dominating process in the water balance of the lake and is approximately 70 % higher than the precipitation falling on the lake. However, the sum of P and inflowing water ($R_{al} + Rs$) exceeds the water mass loss via evaporation processes, resulting in a positive total water balance of the lake and a net rise in lake level for the studied hydrological year. Such a rise would have to continue for another 4–5 consecutive years in order for the lake water to reach a level where surface water outflow from the lake starts to occur.

3.4 Water balance for the TBL catchment

The uncertainty intervals for E, P and R determined above were used in Eq. (4). The ET from the catchment is then calculated to range from 218 690 to 233 750 $m^3\ yr^{-1}$ (185–198 $mm\ yr^{-1}$). In case 1, wind-drifting snow from the lake accumulates on the terrestrial parts of the catchment. P_{land} exceeds the measured P and is equal to $P + P_{winddrift}$. P_{land} is ranging from 306 940–315 210 m^3 (260–267 mm). Based on TDR measurements, ΔS_{al} was estimated to 17 555 m^3 (15 mm). For the terrestrial parts of the catchment the runoff-precipitation (R/P) ratio is approximately 30 %, with the main runoff event occurring during snow melt. The sum of the precipitation falling on the total area of the catchment (lake + terrestrial parts) is higher than the total evapotranspiration, resulting in a positive water balance for the total catchment area.

4 Discussion

4.1 Uncertainty in the water balance

According to the conceptual model for the frozen period (Fig. 5) the only pathway for runoff from the lake is via the talik feature, which could possibly explain the net loss of water calculated for this period in the base case. However, this loss was higher than

HESSD
10, 9271–9308, 2013

allowed for by the considered relevant K value and calculated head gradient between the lake and underlying bedrock. This discrepancy was the basis for the uncertainty analysis performed above. Water loss due to wind drift, sublimation or underestimated groundwater recharge through the underlying talik were considered as possible explanatory processes, not captured in the base case. The resulting uncertainty intervals from the three alternative process cases are based on each additional case process alone compensating for the calculated water loss during the frozen period. However, the latter is most likely a combined effect of different processes. Uncertainties due to measurement errors have further not been analysed in the three scenarios. However, the site data were obtained from sensors with high precision and high time resolution (Table 2), which gives us relatively high confidence in their values and the resulting calculated water balance.

In Fig. 8, the hydraulic heads measured at the lake bottom and in the bedrock during the frozen period are plotted together with the cumulative snow pack (mm SWE). Additionally, two different types of events with strong winds are marked; these are events when the threshold wind speed for snow drift was exceeded, and events when the 5 h mean wind speed exceeded 5 $m s^{-1}$. Based on the change in the lake hydraulic head, the frozen period was subdivided into three consecutive periods, with either an increasing lake pressure head (period 1 and 3) or a decreasing head (period 2). From the graph in Fig. 8, we note that the decrease in lake water head during period 2 co-occurred with a large number of strong wind events, during which mass loss of snow by wind drift and sublimation could be expected. Furthermore, strong wind events were rare in period 1 and 3, and thus the increase in lake level during these periods could primarily reflect accumulation of snow.

The temporal patterns were further examined by comparing change in lake pressure head to wind and relative humidity. For this analysis the data time series were subdivided, splitting each period in half. The change in lake pressure head between the periods was compared to the tested variables listed in Table 5 using linear regression. The analysis shows that a linear combination of two variables could explain

HESSD
10, 9271–9308, 2013

much of the variation in lake level over the six periods ($r^2 = 0.69$). According to this explanation model, lake head decreased when wind speed exceeded the threshold for wind drift ($p = 0.055$) and increased with higher relative humidity during the wind drift events ($p = 0.049$). Although causality cannot be inferred from such correlations, the regression analysis indicates that the hydraulic head change in Two Boat Lake reflects a response to water mass loss due to wind drift and sublimation. The results presented in Fig. 8 together with the regression analysis indicate that a combination of the assumptions in cases 1 and 2 likely explains the identified water loss during the frozen period in the base case.

4.2 Effects of snow sublimation

Snow sublimation has been identified as an important process in cold region hydrology, especially during snow blowing events when the snow is more exposed to sublimation forces (Pomeroy and Gray, 1995; Pomeroy et al., 1997). The number of snow blowing events in the studied area was 106 during the winter 2011–2012, which is in the same range as in other periglacial study sites; in both the Russian Arctic coastal plain and the Colorado alpine region the number of snow blowing events was observed to be over 90 per year (Berg 1986; Groisman et al., 1997). Time-lapse photos also indicate an irregular snow distribution within the catchment. Furthermore, the measured snow depth on the lake ice was smaller than the mean observed snow depth in the catchment.

Reba et al. (2011) measured snow sublimation at a wind-exposed site, with mean daily maximum wind speeds in the same range as at the TBL site, using eddy covariance technique. The measured mean daily sublimation rate for three consecutive snow seasons was then 0.4 mm day^{-1}, corresponding to a total sublimation of 60 mm for the frozen period studied in case 2. This indicates that the calculated evaporation of 40 mm in case 2 is reasonable. Sublimation measurements in the TBL catchment in April 2013 yielded an average value of 2.75 mm day^{-1}. The conditions for sublimation during the observed period were favorable and the result should be interpreted as a maximum

HESSD
10, 9271–9308, 2013

sublimation rate for the frozen period. However, this high measured mass loss shows the importance of quantifying sublimation processes for the water balance of high arctic catchments.

4.3 Hydraulic interactions between lake and underlying bedrock

The co-variation between the pressure head in the lake and that in the borehole below during most of the frozen period (Fig. 8) indicates a good hydraulic contact between the lake and the bedrock. This applies also to the active period when periods of high evapotranspiration and low precipitation cause a decreasing head in the lake, which is also reflected in a falling hydraulic head in the bedrock. The downward pressure gradient between the lake and the bedrock indicates that TBL is underlain by a recharging talik. However, the groundwater recharge flux is small, with the mean Darcy flow velocity over the studied period calculated to be $4.2 \times 10^{-10}\,\mathrm{m\,s^{-1}}$.

Since hydraulic head changes in the bedrock correlate well with pressure changes in the lake, which can in turn be related to near-surface hydrological processes, there are no indications of groundwater discharging into the lake from the unfrozen system below the permafrost. However, it should be noted that groundwater pressure is only monitored in one point below the lake. A model study by Bosson et al. (2010) showed that a talik could act both as a recharge and a discharge area. The TBL catchment is located at high altitude compared to other possible through taliks located further downstream towards the fjord in Kangerlussuaq (Fig. 1). Altitude differences between taliks are important for their recharging or discharging conditions, which has also been shown in previous simulation studies (Bosson et al., 2012b).

The results presented in this work are based on hydrological data only. An analysis of isotopic composition of lake water, groundwater in the active layer and in the borehole is one possible way to further improve the understanding of the hydrological system of the TBL and its catchment. Hydrochemical evaluations of such isotope data could be used to test different parts of the proposed conceptual hydrological model.

HESSD
10, 9271–9308, 2013

5 Conclusions

The annual water balance and intra-annual water balance variability have here been quantified for the hydrological year 1 September 2011 to 31 August 2012 in the Two Boat Lake catchment. This has been achieved by measurement, compilation and analysis of a new, extensive and detailed site-specific dataset with high temporal resolution for key hydrological parameters. Together with a detailed description of geometrical and hydrological properties, this dataset has enabled identification and quantification of main intra-annual processes and hydrological flows in the studied permafrost catchment.

The work highlights the importance of developing a conceptual understanding of hydrological flow variability in a catchment during different time periods within a year. We have shown how this understanding together with the detailed site-specific hydrological data can be used to quantify uncertainty intervals for the different water balance components in a catchment.

Based on the hydrological measurements that link the surface and subsurface water systems below the permafrost, we conclude that the talik below TBL recharges the deeper groundwater. Our results support the hypothesis that relative topographical location governs the direction of groundwater flow in a talik. Temporal pressure changes in the talik closely reflect the measured local hydrological processes at the lake surface rather than any larger-scale regional processes in the ice-sheet dominated landscape. These results indicate catchment hydrology as rather independent from external landscape features, including those of the close-by ice sheet.

We further conclude that sublimation from snow and snowdrift are key processes in the water balance during the frozen period. As a consequence of the snowdrift, the precipitation affecting the catchment differs from that affecting the wind exposed lake area when ice is covering the lake. More generally, the conceptual hydrological model that was developed here entirely from measured site data can contribute valuable input

HESSD
10, 9271–9308, 2013

to further model developments and improve the understanding of permafrost hydrology in periglacial environments.

Supplementary material related to this article is available online at: http://www.hydrol-earth-syst-sci-discuss.net/10/9271/2013/hessd-10-9271-2013-supplement.pdf.

Acknowledgements. This work was conducted within the Greenland Analogue Surface project (GRASP) funded by the Swedish nuclear fuel and waste management Co (SKB). The authors also want to thank the Greenland Analogue Project (GAP) for providing data from DH-GAP01, John Cappelen DMI Denmark for providing meteorological data from Kangerlussuaq and Anders Lindblom, SKB, for help with illustrations.

References

Alexandersson, H.: Korrektion av nederbörd enligt enkel klimatologisk metodik, SMHI Report, No. 111, Swedish Meteorological and hydrological institute, 2003 (in Swedish).

Bense, V. F., Ferguson, G., and Kooi, H.: Evolution of shallow groundwater flow systems in areas of degrading permafrost, Geophys. Res. Lett., 36, L22401, doi:10.1029/2009GL039225, 2009.

Bense, V. F., Kooi, H., Ferguson, G., Read, T.: Permafrost degradation as a control on hydrogeological regime shifts in a warming climate, J. Geophys. Res.-Earth, 117, F03036, doi:10.1029/2011JF002143, 2012.

Berg, N. H.: Blowing snow at a Colorado alpine site: measurements and implications, Arct. Alp. Res., 18, 147–161, 1986.

Bosson, E., Sassner, M., Sabel, U., and Gustafsson, L. G.: Modelling of Present and Future Hydrology and Solute Transport at Forsmark, SR- Site Biosphere, SKB R-10-20, Sven, Kärnbränslehantering AB, Stockholm, 2010.

Bosson, E., Sabel, U., Gustafsson, L.-G., Sassner, M., and Destouni, G.: Influences of shifts in climate, landscape, and permafrost on terrestrial hydrology, J. Geophys. Res., 117, D05120, doi:10.1029/2011JD016429, 2012a.

HESSD

10, 9271–9308, 2013

Bosson, E., Selroos, J.-O., Stigsson, M., Gustafsson, L.-G., and Destouni, G.: Exchange and pathways of deep and shallow groundwater in different climate and permafrost conditions using the Forsmark site, Sweden, as an example catchment, Hydrogeol. J., 21, 225–237, doi:10.1007/s10040-012-0906-7, 2012b.

Cappelen, J. (Ed.): Weather and climate data from Greenland 1958–2011 – observation data with description, DMI Technical Report 12–15, Danish meteorological institute, 2012.

Cheng, G. and Jin, H.: Permafrost and groundwater on the Qinghai-Tibet Plateau and in north-east China, Hydrogeol. J., 21, 5–23, doi:10.1007/s10040-012-0927-2, 2012.

Clarhäll, A. (Ed.): SKB studies of the periglacial environment – report from field studies in Kangerlussuaq, Greenland 2008 and 2010, P-11-05, Svensk Kärnbränslehantering AB, 2011.

Engels, S. and Helmens, K.: Holocene environmental changes and climate development in Greenland, SKB R-10-65, Svensk Kaärnbraänslehantering AB, 2010.

Frampton, A., Painter, S., Lyon, S. W., and Destouni, G.: Non-isothermal, three-phase simulations of near-surface flows in a model permafrost system under seasonal variability and climate change, J. Hydrol., 403, 352–359, doi:10.1016/j.jhydrol.2011.04.010, 2011.

Frampton, A., Painter, S., Lyon, S. W., and Destouni, G.: Permafrost degradation and subsurface-flow changes caused by surface warming trends, Hydrogeol. J., 21, 271–280, doi:10.1007/s10040-012-0938-z, 2012.

Førland, E. J., Allerup, P., Dahlström, B., Elomaa, E., Jonsson, J., Madsen, H., Perälä, J., Rissanan, P., Vedin, H., and Vejen, F.: Manual for Operational Correction of Nordic Precipitation Data, DNMI Report no. 24/96, Norwegian Meteorological Institute, 1996.

Ge, S., McKenzie, J., Voss, C., and Wu, Q.: Exchange of groundwater and surface-water mediated by permafrost response to seasonal and long term air temperature variation, Geophys. Res. Lett., 38, L14402, doi:10.1029/2011GL047911, 2011.

Grenier, C., Régnier, D., Mouche, E., Benabderrahmane, H., Costard, F., and Davy, P.: Impact of permafrost development on groundwater flow patterns: a numerical study considering freezing cycles on a two-dimensional vertical cut through a generic river-plain system, 21, 257–270, doi:10.1007/s10040-012-0909-4, 2012.

Groisman, P. Y., Golubev, V. S., Genikhovich, E. L., and Bomin., S.: Evaporation from Snow Cover: An empirical study, Proc. Conf. on Polar Processes and Global Climate, Rosario, WA, ACSYS, 72–73, 1997.

HESSD
10, 9271–9308, 2013

Harper, J., Hubbard, A., Ruskeeniemi, T., Claesson Liljedahl, L., Lehtinen, A., Booth, A., Brinkerhoff, D., Drake, H., Dow, C., Doyle, S., Engström J., Fitzpatrik, A., Frape, S., Henkemans, E., Humphrey, N., Johnson, J., Jones, G., Joughin, I., Klint, K. E., Kukkonen, I., Kulessa, B., Londowski, C., Lindbäck, K., Makahnouk, M., Meierbachtol, T., Pere, T.,Pedersen, K., Petterson, R., Pimentel, S., Quincey, D., Tullborg, E.-L., and van As, D.: The Greenland Analogue Project Yearly Report 2010, Swedish Nuclear Fuel and Waste Manage Co. Report SKB R-11-23, 2011.

Hasholt, B.: Runoff patterns in Greenland, Northern Research Basins: Proc. 11th Int. Symp., and Workshop, Vol. 1, Fairbanks, AK, 71–81, 1997.

Helbig, M., Boike, J., Langer, M., Schreiber, P., Runkle, B. R. K., and Kutzbach, L.: Spatial and seasonal variability of polygonal tundra water balance: Lena River Delta, northern Siberia (Russia), Hydrogeol. J., 21, 133–147, doi:10.1007/s10040-012-0933-4, 2012.

Hinzman, L. D., Destouni, G., and Woo, M. K.: Preface: hydrogeology of cold regions, Hydrogeology J., 21, 1–4, doi:10.1007/s10040-012-0943-2, 2012.

Hirashima, H., Ohata, T., Kodama, Y., and Yabuki, H.: Estimation of annual water balance in Siberian tundra using a new land surface model, Northern Research Water balance, IAHS Publication 290, ISSN 0144-7815, 2004.

Hiroyuki, H., Tetsou, O., Yuji, K., and Hironori, Y.: Estimation of annual water balance in Siberian tundra using a new land surface model, Northern research Basins Water Balance, IAHS Publication 290, ISSN 0144-7815, 2004.

Kane, D. L. and Yang, D. (Eds.): Overview of water balance determinations for high latitude watersheds, in: Northern Research Basins Water Balance, International Association of Hydrological Sciences, IAHS Publ., Publication 290, ISSN 0144-7815, Wallingford, UK, 271 pp., 2004.

Kane, D. L., Yoshikawa, K., and McNamara, J. P.: Regional groundwater flow in an area mapped as continuous permafrost, NE Alaska (USA), Hydrogeol. J., 21, 41–52, 2012.

Lyon, S. W., Mörth, M., Humborg, C., Giesler, R., and Destouni, G.: The relationship between subsurface hydrology and dissolved carbon fluxes for a sub-arctic catchment, Hydrol. Earth Syst. Sci., 14, 941–950, doi:10.5194/hess-14-941-2010, 2010.

Li, L. and Pomeroy, J.-W.: Estimates of threshold wind speeds for snow transport using meteorological data, J. Appl. Meteorol., 36, 205–213, doi:10.1175/1520-0450(1997)036¡0205:EOTWSF¿2.0.CO;2 1997.

HESSD
10, 9271–9308, 2013

MacDonald, M. K., Pomeroy, J. W., and Pietroniro, A.: On the importance of sublimation to an alpine snow mass balance in the Canadian Rocky Mountains, Hydrol. Earth Syst. Sci., 14, 1401–1415, doi:10.5194/hess-14-1401-2010, 2010.
McKenzie, J. M. and Voss, C. I.: Permafrost thaw in a nested groundwater-flow system, Hydrogeol. J., 21, 299–316, doi:10.1007/s10040-012-0942-3, 2012.
Penman, H. L.: Natural evaporation from open water, bare soil and grass, P. R. Soc. London, 193, 120–145, 1948.
Petrone, J.: Using ground-penetrating Radar to Estimate Sediment Load in and Around TwoBoatLake, Western Greenland, (Student paper), Uppsala universitet, 2013.
Pomeroy, J. W. and Gray, D. M.: Snowcover Accumulation, Relocation and Management, National Hydrological Research Institute Science Report, 7, Environment Canada, Saskatoon, Canada, 144 pp., 1995.
Pomeroy, J. W., Marsh, P., and Gray, D. M.: Application of a distributed blowing snow model to the Arctic, Hydrol. Process., 11, 1451–1464, 1997.
Quinton, W. L. and Baltzer, J. L.: The active-layer hydrology of a peat plateau with thawing permafrost (Scotty Creek, Canada), Hydrogeol. J., 21, 201–220, doi:10.1007/s10040-012-0935-2, 2012.
Quinton, W. L. and Carey, S. K.: Towards an energy-based runoff generation theory for tundra landscapes, Hydrol. Process., 22, 4649–4653, doi:10.1002/hyp.7164, 2008.
Reba, M. L., Pomeroy, J., Marks, D., and Link, T. E.: Estimating surface sublimation losses from snowpacks in a mountain catchment using eddy covariance and turbulent transfer calculations, Hydrol. Process., 26, 3699–3711, doi:10.1002/hyp.8372, 2011.
Sjöberg, Y., Frampton, A., and Lyon, S. W.: Using streamflow characteristics to explore permafrost thawing in northern Swedish catchments, Hydrogeol. J., 21, 121–131, doi:10.1007/s10040-012-0932-5, 2012.
Wellman, T. P., Voss, C. I., and Walvoord, M. A.: Impacts of climate, lake size, and supra- and sub-permafrost groundwater flow on lake-talik evolution, Yukon Flats, Alaska (USA), Hydrogeol. J., 21, 281–298, doi:10.1007/s10040-012-0941-4, 2012.
White, D., Hinzman, L., Alessa, L., Cassano, J., Chambers, M., Falkner, K., Francis, J., Gutowski Jr., W. J., Holland, M., Holmes, R. M., Huntington, H., Kane, D., Kliskey, A., Lee, C., McClelland, J., Peterson, B, Rupp, T. S., Straneo, F., Steele, M., Woodgate, R., Yang, D., Yoshikawa, K., and Zhang, T.: The arctic freshwater system: changes and impacts, J. Geophys. Res., 112, G04S54, doi:10.1029/2006JG000353, 2007.

HESSD
10, 9271–9308, 2013

Willemse, N. W., Koster, E. A., Hoogakker, B., and van Tatenhove, F. G. M.: A continuous record of Holocene eolian activity in West Greenland, Quaternary Res., 59, 322–334, 2003.
Woo, M. K.: Permafrost hydrology in North America, Atmos. Ocean, 24, 201–234, 1986.
Woo, M.-K., Kane, D. L., Carey, S. K., and Yang, D.: Progress in permafrost hydrology in the new millennium, Permafr. Periglac. Process., 19, 237–254, 2008.

HESSD
10, 9271–9308, 2013

Table 1. Geometrical parameters for TBL catchment.

Catchment area, km^2	1.56
Lake area, km^2	0.377
Lake fraction, %	24
Catchment relief max, m	505
Catchment relief min, m	337
Lake maximum depth, m	29.9
Lake mean depth, m	11.3
Lake volume (Sep 2010), Mm^3	4.29

HESSD
10, 9271–9308, 2013

Table 2. Monitored data, type of equipment, available data period and logging interval for installations in the Two Boat Lake catchment. The accuracy of the sensors for each monitored parameter is also listed.

Station	Parameter	Equipment	Monitoring started	Time resolution	Accuracy
AWS	Wind direction	R.M.Young, 05103-45	Apr 2011	10 min	±3°
AWS	Wind speed	R.M.Young, 05103-45	Apr 2011	10 min	±0.3 m s^{-1}
AWS	Ingoing longwave radiation	Kipp & Zonen, CNR4	Apr 2011	10 min	5–10 µV/W m^{-2}
AWS	Outgoing longwave radiation	Kipp & Zonen, CNR4	Apr 2011	10 min	5–10 µV/W m^{-2}
AWS	intgoing shortwave radiation	Kipp & Zonen, CNR4	Apr 2011	10 min	7 to 20 µV/W m^{-2}
AWS	Outgoing shortwave radiation	Kipp & Zonen, CNR4	Apr 2011	10 min	7 to 20 µV/W m^{-2}
AWS	Relative humidity	HygroclipS3	Apr 2011	10 min	1.5 % RH
AWS	Air temperature	Rotronic, MP100H-4-1-03-00-10DIN	Apr 2011	10 min	0.1 °C
AWS	Precipitation	Geonor T-200B	Apr 2011	10 min	0.1 %
AWS	Barometric pressure	Setra, CS100-Setramodel278	Apr 2011	10 min	±0.5mbar
Soil temperature	Soil temperature	HOBO	Aug 2010	3 h	±0.25 °C
TDR	Soil moisture	cs615, CR1000	Aug 2010	3 h	±2 %
Time lapse camera	Snow events, lake freezing	Canon Rebel T3 (1100D) /Harbortronics DigiSnap 2700	Apr 2011/Aug 2012	0.5 h/2 h	
DH GAP-01	*T*, *P*, EC	Aqua troll 200	Sep 2010	15 min–12 h	±0.1 %
Lake Water level	Water pressure	Level troll 700	Aug 2010	3 h	±0.1 %

HESSD
10, 9271–9308, 2013

Table 3. Data on total Precipitation (*P*), Potential evapotranspiration (PET) and Air temperature from the Automatic weather station (AWS) and from the station in Kangerlussuaq. The listed precipitation values are corrected values, the applied correction factors for wind and adhesion losses are listed in the end of the table. The total *P* is also given as snow and rain for each month.

AWS at TBL Catchment 2011	Rain[b], mm	Snow[b], mm	Total *P*, mm	PET, mm	Air Temperature, °C
May	1.1	9.9	11.1	65.8	−1.4
Jun	1.4	0.0	1.4	112.3	7.0
Jul	19.4	0.0	19.4	112.9	9.0
Aug	20.3	0.0	20.3	66.2	7.2
Sep	7.0	2.6	9.6	25.6	0.8
Oct	1.7	13.8	15.5	3.1	−7.9
Nov	4.4	10.6	15.0	3.7	−11.5
Dec	0.4	14.6	15.0	4.2	−13.7
2012	**Rain[b], mm**	**Snow[b], mm**	**Total *P*, mm**	**PET, mm**	**Air Temperature, °C**
Jan	0.0	7.6	7.6	4.7	−16.1
Feb	0.5	9.1	9.5	1.9	−15.0
Mar	1.4	7.8	9.2	4.3	−18.3
Apr	16.9	31.4	48.3	25.3	−4.0
May	23.3	12.6	35.9	76.9	3.0
Jun	19.7	0.0	19.7	102.1	8.2
Jul	24.4	0.0	24.4	102.4	9.2
Aug	50.2	0.0	50.2	59.1	7.2
Sep	83.5	0.3	83.8	24.8	2.9
Oct	15.6	26.3	42.0	14.0	−2.0
Nov	0.0	28.0	28.0	X	−10.2
Dec	0.0	13.0	14.3	X	−12.4
Annual sum	*236*	*136*	*372*	X	Annual mean temp: −4.0
Sum HY[a]	*150*	*110*	*260*	*413*	Mean temp HY[a]: −4.8
DMI Station Kangerlussuaq					
	Rain[b], mm	**Snow[b], mm**	**Total *P*, mm**	**PET, mm**	**Air Temperature°C**
Annual sum 2012	257	89	346	X	Annual mean temp: −4.1
Sum HY[a]	130	55	185	X	Mean temp HY[a]: −4.7

[a] HY = Hydrological year 1 Sep 2011 –31 Aug 2012
[b] Precipitation is corrected with following factors:
Kangerlussuaq: Snow 16 %, Rain 4.5 %. Adhesion losses 0.1 mm/precipitation event
AWS: Snow 33 %, Rain 12 %. Adhesion losses 0.1 mm/precipitation event

HESSD
10, 9271–9308, 2013

Table 4. Periods of thawing and freezing, and active and frozen conditions of the active layer, for the studied hydrological year. The conditions for the lake ice for each period are also listed in the table.

Conditions of soil in active layer	Time of the year	Lake ice dynamics
Active Period	May–Oct	Ice free Jun–Sep
Frozen period	Nov–Apr	Lake ice thicker than active layer, maximum thickness 1.6 m
Freezing period	Oct	Lake freeze
Thawing period	May	Lake thaw

HESSD
10, 9271–9308, 2013

Table 5. Definitions of periods analyzed in the correlation analysis. For each period the net change in lake pressure head (ΔH), number of events with strong winds (wind speed > threshold wind speed for snow drift (th_wd) and wind speed > 5 m s^{-1}), and the relative humidity (RH) are given. The mean RH for each period as well as the mean RH during events when wind speed exceeded th_wd are listed in the table. In the correlation analysis the number of wind events with windspeed > th_wd and RH was used as input variables.

			Wind events		RH, %	
Period	Start	ΔH, mm	> th_wd	> 5 m s^{-1}	RH when windspeed > th_wd	mean RH for period
1a	1 Nov 2011	−2.9	4	21	50.3	72.4
1b	18 Nov 2011	6.6	0	33	0.0	74.0
2a	5 Dec 2011	−12.2	40	153	59.8	70.7
2b	3 Jan 2012	−6.5	35	132	54.4	72.0
3a	2 Feb 2012	20.4	7	83	88.4	78.1
3b	1 Mar 2012	9.9	11	68	64.7	75.3

HESSD
10, 9271–9308, 2013

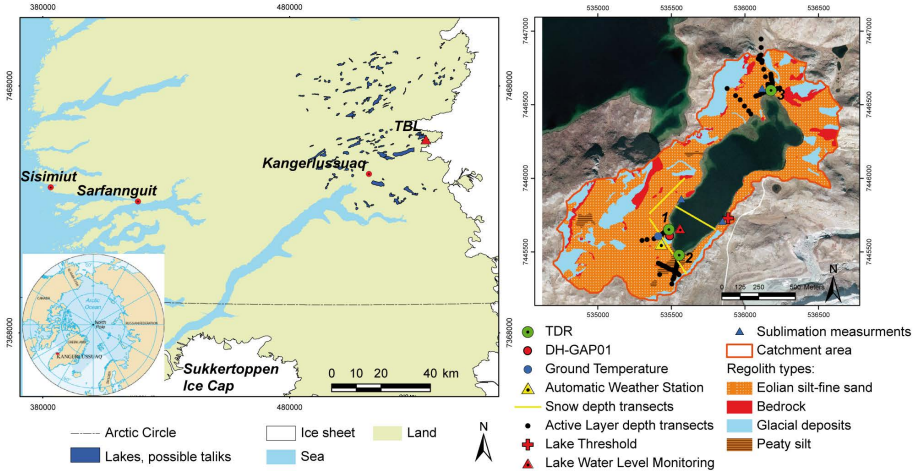

Fig. 1. Location of the Kangerlussuaq settlement and the Two Boat Lake catchment, left. In the left figure possible talik locations (in the Kangerlussuaq region) and the Greenland Ice Sheet are also marked. The right figure shows the map of the regolith distribution in the TBL catchment together with the monitoring points and transects for measurements of active layer depth and snow depth.

HESSD
10, 9271–9308, 2013

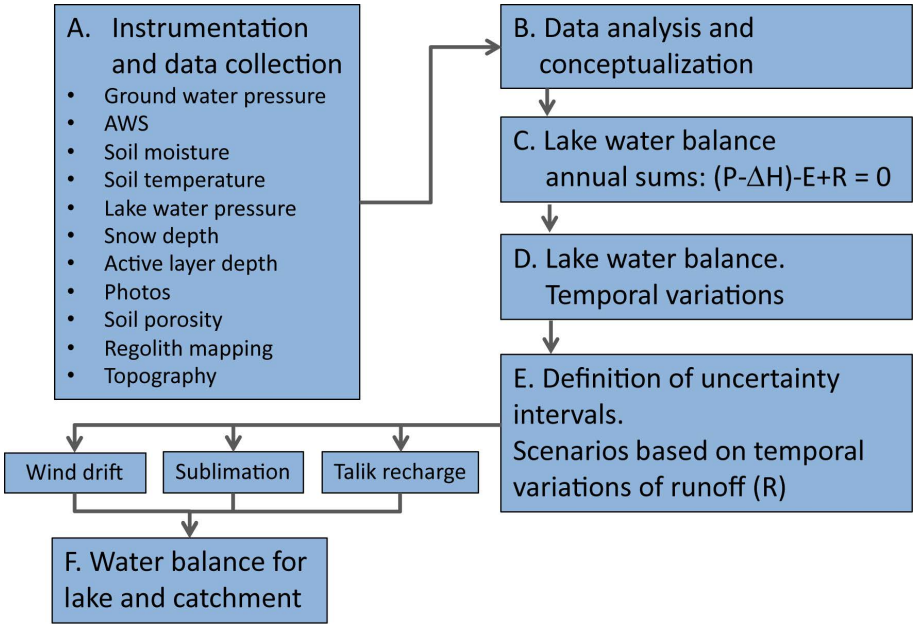

Fig. 2. Overall method and workflow, step A–F, for water balance calculations and conceptualisation of the hydrology in the Two Boat Lake catchment.

HESSD
10, 9271–9308, 2013

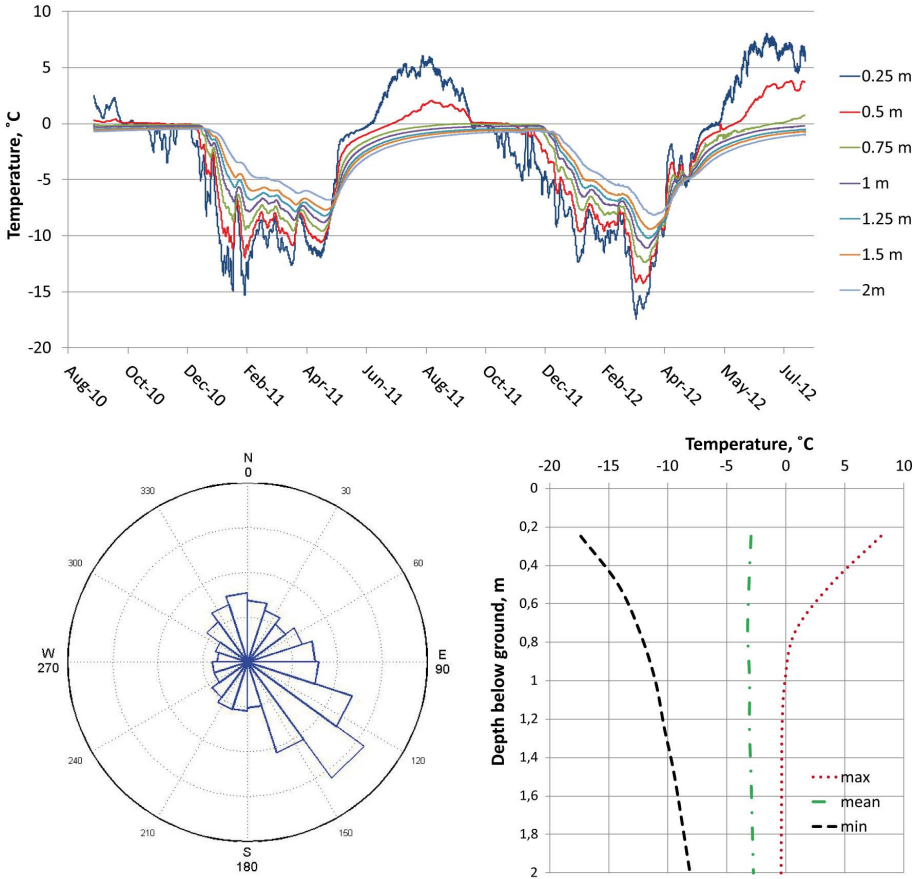

Fig. 3. Soil temperature data for the observed period at different depths below ground (Upper figure) and min, max and mean temperatures at each depth for the observed period observed (lower right). The lower left figure illustrates the dominating wind direction coming from south east.

HESSD
10, 9271–9308, 2013

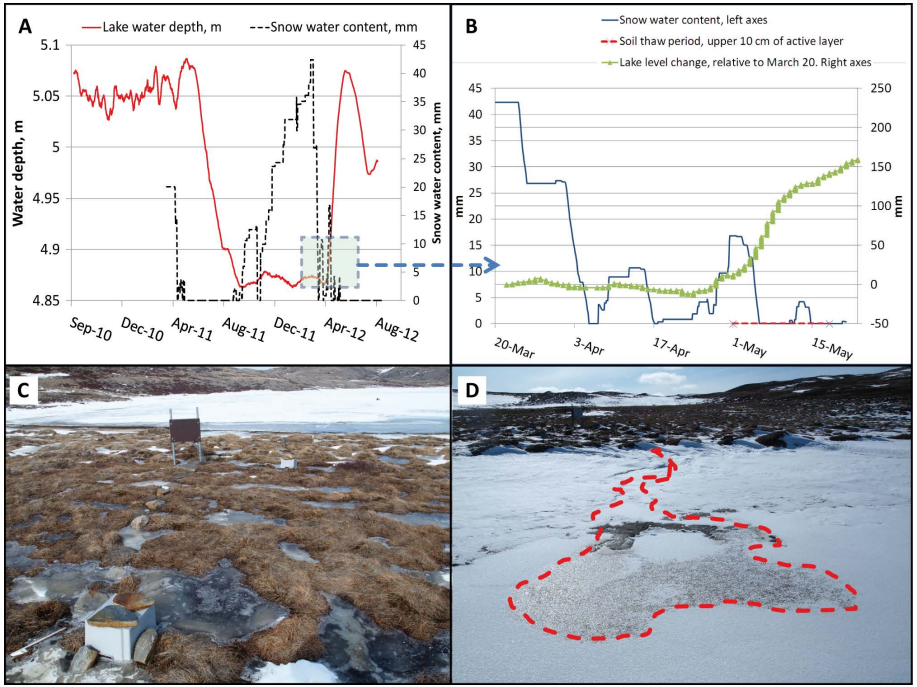

Fig. 4. Lake level fluctuation (red line) and snow accumulation/melt (black dotted line) for the observed period **(A)**. In **(B)** the lake level fluctuation during snow melt and soil thaw in spring 2012 is illustrated. Snow melt in early spring building ponds at the frozen ground surface **(C)**. As the soil surface thaws the water in the ponds melts, the water becomes mobile and is transported towards the lake **(D)**.

HESSD
10, 9271–9308, 2013

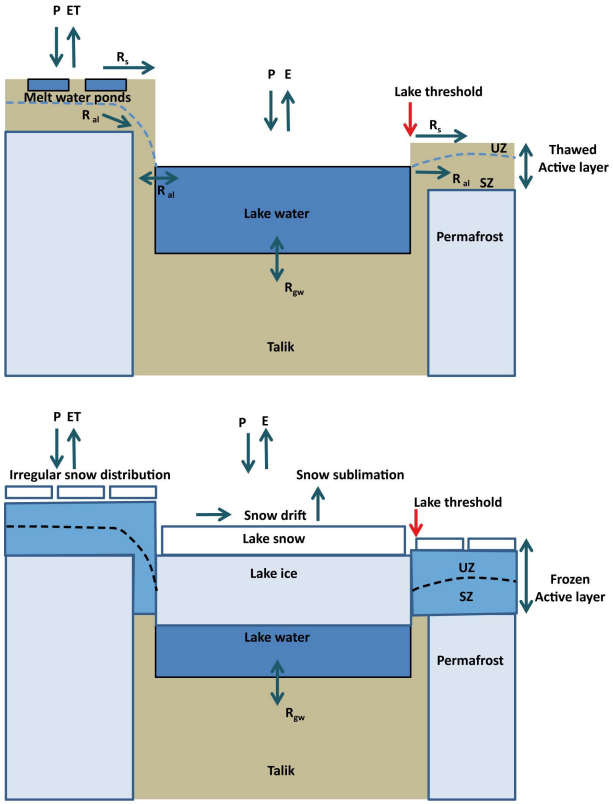

Fig. 5. Conceptual model of the hydrological flows during the active (upper figure) and frozen period (lower figure) in the Two Boat Lake catchment. The conditions for precipitation (P), evaporation (E) and evapotranspiration (ET) as well as runoff from active layer (R_{al}), water exchange with the talik (R_{gw}), and surface water runoff (Rs) are illustrated. The unsaturated and saturated zones are denoted UZ and SZ respectively. The blue arrows illustrate the main hydrological flows for each period and the red arrow indicates the location of the lake threshold for surface water outflow.

HESSD
10, 9271–9308, 2013

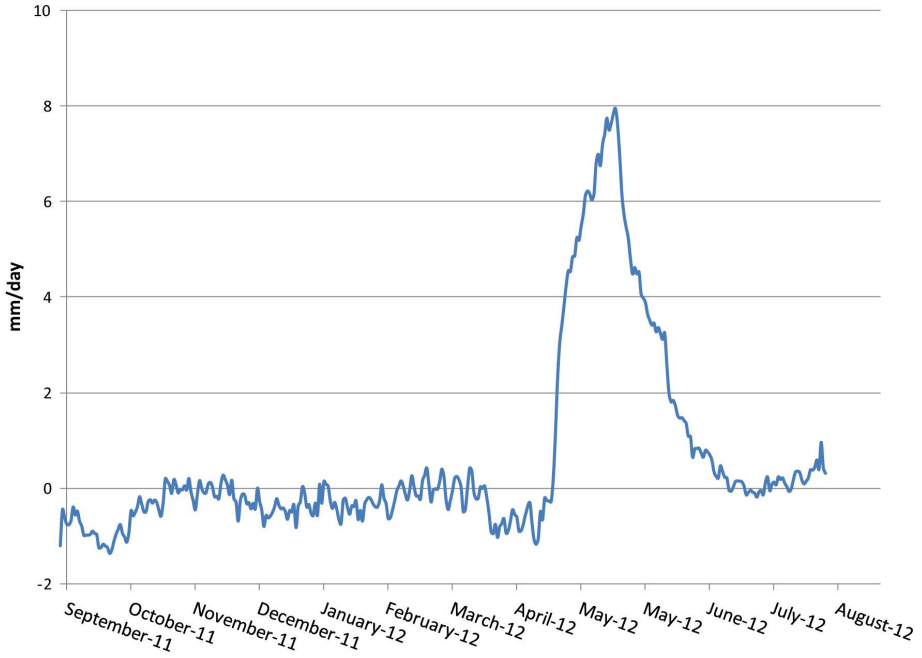

Fig. 6. Calculated total runoff, mm day^{-1}, from time series of precipitation (P), Potential evapotranspiration (PET) and change in lake level (ΔH).

HESSD
10, 9271–9308, 2013

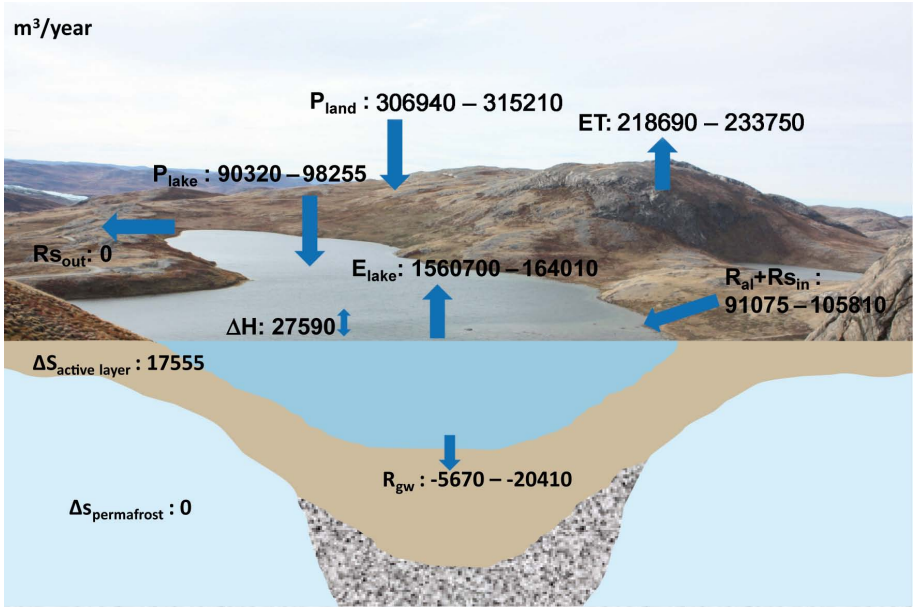

Fig. 7. Water balance, $m^3 yr^{-1}$, for the Two Boat Lake catchment based on data from the hydrological year 1 September 2011 until 31 August 2012. Due to snow drift in the area different values of precipitation, P_{land} and P_{lake}, are calculated. Uncertainty intervals are presented for the evaporation (E_{lake}) and evapotranspiration (ET), precipitation (P_{lake} and P_{land}) and runoff (R_{gw} and $R_{al} + Rs_{in}$) components. Uncertainty intervals are not defined for the change in lake level (ΔH) and storage change in the active layer (ΔS).

HESSD
10, 9271–9308, 2013

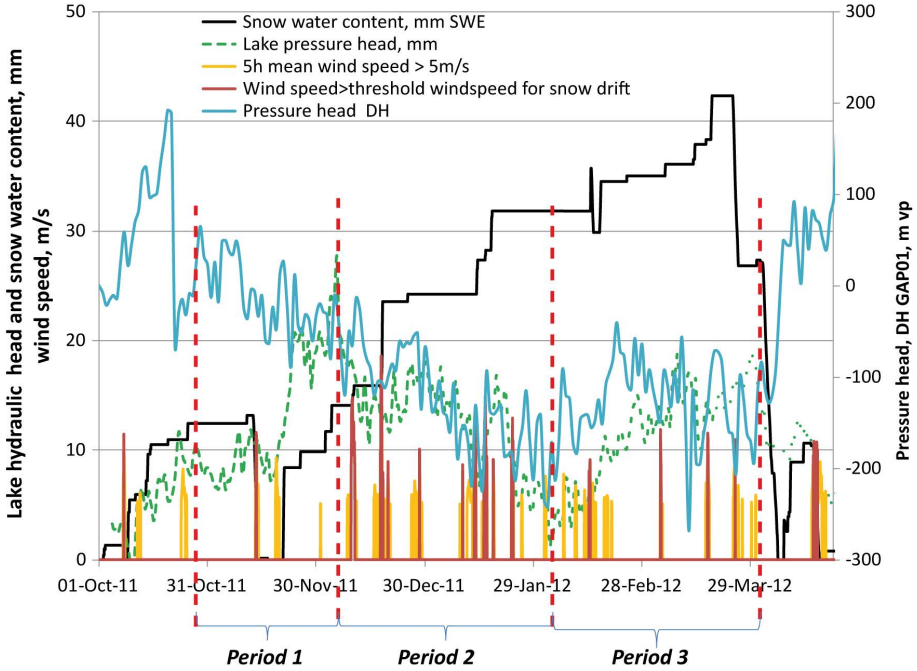

Fig. 8. Pressure head in lake (green dotted line) and bedrock (blue line) co-plotted with cumulative snowpack (black line) and events of strong winds (events when the 5 h mean wind speed $> 5\,m\,s^{-1}$ and events when the wind speed exceeded the threshold wind speed for snow drift, $7\,m\,s^{-1}$). Lake hydraulic head and cumulative snowpack in mm and wind speed in $m\,s^{-1}$ are plotted on the left axes and pressure head in the bedrock, m vp, plotted on the right axes. Data is illustrated for the frozen period 2011–2012. The frozen period is divided into 3 periods, 1–3, based on an increasing or decreasing trend in lake head.

HESSD
10, 9271–9308, 2013